Elsevier Editorial System(tm) for Energy
Manuscript Draft

Manuscript Number: EGY-D-13-02586R1

Title: Passive intensification of the ammonia absorption process with NH3/LiNO3 using carbon nanotubes and advanced surfaces in a tubular bubble absorber

Article Type: Full Length Article

Keywords: Bubble absorber, carbon nanotubes, advanced surfaces, ammonia, lithium nitrate.

Corresponding Author: Prof. Mahmoud Bourouis, Ph.D.

Corresponding Author's Institution: Rovira i Virgili University

First Author: Carlos Amaris, Ph.D Student

Order of Authors: Carlos Amaris, Ph.D Student; Mahmoud Bourouis, Ph.D.; Manel Vallès, Ph.D

Abstract: The present study aims to quantify experimentally the individual and simultaneous effects of carbon nanotubes (CNTs) and advanced surfaces on the performance of an NH3/LiNO3 tubular bubble absorber. Operating conditions are those of interest for use in air-cooled absorption chillers driven by low temperature heat sources. Firstly, experimental tests were performed with the tubular absorber fitted with an inner smooth surface to analyse the effect of adding carbon nanotubes (0.01wt %) to the base mixture NH3/LiNO3. Then, the tubular absorber was tested using an inner advanced surface tube both with and without adding carbon nanotubes to the base mixture NH3/LiNO3. The advanced surface tube is made of aluminium and has internal helical micro-fins measuring 0.3 mm in length. Results show that the maximum absorption mass flux achieved with the CNT binary nanofluid and the smooth tube is up to 1.64 and 1.48 times higher than reference values at cooling-water temperatures of 40 and 35 ºC, respectively. It is also found that simultaneous use of CNT nanoparticles and advanced surfaces resulted in a more pronounced increase in the absorption mass flux and solution heat transfer coefficient with respect to the smooth tube absorber with NH3/LiNO3 as a working pair.

Passive intensification of the ammonia absorption process with $NH_3/LiNO_3$ using carbon nanotubes and advanced surfaces in a tubular bubble absorber

Carlos Amaris, Mahmoud Bourouis* and Manel Vallès

CREVER – Universitat Rovira i Virgili, Av. Països Catalans No. 26,

43007 Tarragona, Spain.

*Corresponding author Email: mahmoud.bourouis@urv.cat ; Phone +34 977 55 86 13

Mailing address: Universitat Rovira I Virgili, Av. Països Catalans, 26, 43007,

Tarragona (Spain)

ABSTRACT

The present study aims to quantify experimentally the individual and simultaneous effects of carbon nanotubes (CNTs) and advanced surfaces on the performance of an $NH_3/LiNO_3$ tubular bubble absorber. Operating conditions are those of interest for use in air-cooled absorption chillers driven by low temperature heat sources. Firstly, experimental tests were performed with the tubular absorber fitted with an inner smooth surface to analyse the effect of adding carbon nanotubes (0.01wt %) to the base mixture $NH_3/LiNO_3$. Then, the tubular absorber was tested using an inner advanced surface tube both with and without adding carbon nanotubes to the base mixture $NH_3/LiNO_3$. The advanced surface tube is made of aluminium and has internal helical micro-fins measuring 0.3 mm in length.

Results show that the maximum absorption mass flux achieved with the CNT binary nanofluid and the smooth tube is up to 1.64 and 1.48 times higher than reference values at cooling-water temperatures of 40 and 35 ºC, respectively. It is also found that simultaneous use of CNT nanoparticles and advanced surfaces resulted in a more pronounced increase in the absorption mass flux and solution heat transfer coefficient with respect to the smooth tube absorber with $NH_3/LiNO_3$ as a working pair.

Keywords: Bubble absorber, carbon nanotubes, advanced surfaces, ammonia, lithium nitrate.

Highlights

- We experimentally studied the passive intensification of the ammonia absorption process with the $NH_3/LiNO_3$ mixture in a tubular bubble absorber.
- We analyzed the effect of carbon nanotubes (CNTs) and advanced surfaces on the absorber performance working with $NH_3/LiNO_3$.
- The use of CNT binary nanofluid in the smooth tube significantly increased the absorption mass flux compared with $NH_3/LiNO_3$.
- The simultaneous use of CNT nanoparticles and advanced surfaces resulted in a more pronounced enhancement of the absorption mass flux.

Nomenclature

A	*heat transfer area, m^2*
C	*correction factor*
Cp	*heat capacity, $kJ.kg^{-1}.K^{-1}$*
D	*diameter, m*
f	*friction factor*
F	*ammonia absorption mass flux, $kg.m^{-2}.s^{-1}$*
h	*heat transfer coefficient, $kW.m^{-2}.K^{-1}$*
k	*thermal conductivity, $kW.m^{-1}.K^{-1}$*
LMTD	*logarithmic mean temperature difference, ºC*
$\dot{m}$	*mass flow rate, $kg.s^{-1}$*
Nu	*Nusselt number*
OD	*outer diameter, m*
Pr	*Prandtl number*
Q	*thermal load per unit of area, $kW.m^{-2}$*
Q_{AB}	*thermal load, kW*
Re	*Reynolds number*
U	*overall heat transfer coefficient, $kW.m^{-2}.K^{-1}$*
V	*volumetric flow rate, $l.h^{-1}$*
T	*temperature, ºC*
P	*pressure, kPa*

Subscripts:

AB	*absorber*
Al	*aluminum*
CNTs	*carbon nanotubes*
Cw	*cooling-water*

Eq *equilibrium*

In *absorber inlet*

Inner *inner diameter of the tube*

NH_3 *ammonia*

o *outer tube*

Out *absorber outlet*

Outer *outer diameter of the tube*

Sat *saturation state*

Sol *solution of $NH_3/LiNO_3$*

Sub *subcooling*

Greek letters:

ΔT *temperature difference, ºC*

ΔP *total pressure drop, kPa*

ρ *density*

1. Introduction

The potential of absorption refrigeration cycles driven by residual heat or solar thermal energy has been recognized for a long time. Over the last years, the interest and necessity to progress in the development of absorption chillers have led to studies of several techniques to improve their performances and make them more competitive than mechanical compression systems. Current research on absorption chillers is essentially focused on the study and development of new cycles and of new working fluids.

Well-known drawbacks of the conventional working fluids for absorption refrigeration systems such as crystallization, corrosion and low operating pressures for $H_2O/LiBr$ cycles and refrigerant vapor rectification at the desorber outlet for NH_3/H_2O cycles have increased the interest of researchers in new working mixtures. Investigations with the $NH_3/LiNO_3$ mixture have resulted in this mixture being considered a promising alternative working pair for absorption refrigeration cycles driven by low temperature heat sources (Gensch [1], Aggarwal and Agarwal [2] and Infante Ferreira [3]).

Refrigeration systems with $NH_3/LiNO_3$ as the working fluid can be air-cooled since high condensation temperatures can be achieved without crystallization problems. They also can be operated at low generator temperatures and refrigerant vapor rectification at the generator outlet is not needed (Antonopoulos et al. [4], Sun [5], Abdulateef et al. [6] and Infante Ferreira [7]). Accordingly, refrigeration systems with $NH_3/LiNO_3$ are highly

recommended for solar cooling applications. However, previous experimental studies showed that the main drawback of $NH_3/LiNO_3$ is its high viscosity, which limits heat and mass transfer processes in the absorber, as compared to the use of NH_3/H_2O working fluid (Abdulateef et al. [6], Infante Ferreira [7], Ayala et al. [8], Heard et al. [9]).

Regarding the most recent experimental research works with $NH_3/LiNO_3$, studies on the boiling heat transfer in plate heat exchangers have been reported by Oronel et al. [10], Zacarías et al. [11] and Venegas et al. [12]. Oronel et al. [10] reported an experimental study on the saturated boiling process in a plate heat exchanger for $NH_3/LiNO_3$ and $NH_3/(LiNO_3+H_2O)$ working fluids. The authors analyzed the different boiling regimes (convective, nucleate and film boiling) that take place as well as the effect of operating parameters such as mean vapor quality, heat flux and solution mass flux on the boiling heat transfer coefficient for both $NH_3/LiNO_3$ and $NH_3/(LiNO_3+H_2O)$. Meanwhile, Herrera et al. [13] performed an experimental and numerical study on the performance of a horizontal tube falling film generator operating in a 10 kW $NH_3/LiNO_3$ absorption refrigeration prototype. The falling film generator was made of carbon steel and operated at a pressure of 15.56 bar.

In 2011, Bourouis et al. [14] obtained the first patent for a water-cooled or air-cooled single-stage absorption chiller using $NH_3/LiNO_3$ for solar cooling applications. These absorption chillers have as the main characteristic the use of brazed plate heat exchangers in all components. In the same year, Rivera et al. [15] evaluated experimentally the performance of an intermittent refrigeration system operating with a $NH_3/LiNO_3$ mixture. The system developed has a nominal capacity of 8 kg of ice/day and was capable to obtain evaporation temperatures as low as -11 ºC. Llamas et al. [16] reported experimental results of an air-cooled 5 kW $NH_3/LiNO_3$ absorption cooling prototype driven by solar energy. COP values reported a range between 0.35 and 0.4.

Zacarías et al. [17] conducted an experimental evaluation of an adiabatic absorber working with the $NH_3/LiNO_3$ mixture using a flat fan nozzle at the absorber top and a plate heat exchanger as a sub-cooler for the solution coming from the generator. Similarly, Ventas et al. [18] and Zacarías et al. [19] reported experimental results of the adiabatic absorption process with the $NH_3/LiNO_3$ mixture using a fog-jet injector. Moreno-Quintanar et al. [20] published the experimental performance of a solar powered intermittent absorption refrigeration system with both $NH_3/LiNO_3$ and $NH_3/(LiNO_3+H_2O)$ for ice production. In this study, it was found that at some operating

conditions the solar coefficients of performance using the $NH_3/(LiNO_3+H_2O)$ mixture were up to 24 % higher than those obtained with the $NH_3/LiNO_3$ mixture and that the initial generation temperatures were up to 5.5 ºC lower than those required for the $NH_3/LiNO_3$ mixture.

Studies employing intensification techniques to improve heat and mass transfer processes in the absorber, such as mechanical treatments, i.e. scratching tube surfaces to increase surface roughness and the use of advanced surface, or the addition of small quantities of a surfactant, which causes interfacial turbulence, to working fluids have been carried out more frequently in over the last years. Recently, optimization of nanoparticles synthesis and reduction in the acquisition prices has also allowed for the inclusion of nanotechnology in absorption refrigeration systems as a technique for enhancing heat and mass transfer processes. In this case, the working fluid is usually called binary nanofluid, which means binary mixture with nano-sized particles.

Studies on absorption process with advanced surfaces may include the use of plate heat exchangers. Kang et al. [21] characterized the absorption process and reported correlations for heat and mass transfer with NH_3/H_2O mixture in a plate heat exchanger with enhanced surfaces such as offset strip fin (OSF) and falling film configuration. Furthermore, Cerezo et al. [22] carried out an experimental characterization of a corrugated three channel plate heat exchanger as a bubble absorber with NH_3/H_2O and compared the results with those achieved by using a theoretical model.

Intensification of the absorption process in a H_2O/LiBr falling film on horizontal tubes using several advanced surfaces, hatched tubes and surfactants has also been reported in the literature (Miller [23], Yoon et al. [24] and Park et al. [25]). These studies showed that improvements stemming from the use of mechanical treatments were not as high as enhancements induced by the chemical agitation of surfactants and that the synergistic effects were rather small.

Experiments on the effect of nanoparticles (CNTs, SiO_2) in the H_2O/LiBr solution employed as working pair in falling film absorbers have also been evaluated (Kim et al. [26] and Kang et al. [27]). The results showed that adding CNTs particles to the H_2O/LiBr solution significantly increases mass transfer rates, up to about 2.48 times for a nanoparticles concentration of 0.1 wt. % [26].

Several experimental studies employing an NH_3/H_2O mixture as the working pair have also been reported in the literature. Kim et al. [28, 29] studied the effect of different kinds of nanoparticles (Cu, CuO, and Al_2O_3) and surfactants on the absorption rate in

bubble mode without heat removal. Results showed that NH_3/H_2O with 2-Ethyl-1-hexanol as surfactant and Cu nanoparticles at 0.1 wt. % presented the highest increase of the absorption rate (5.32 times higher than reference values) at the highest concentration of ammonia employed. Similar experimental studies on bubble absorbers with NH_3/H_2O and many kinds of nanoparticles (CNTs, Al_2O_3 and Ag) were carried out and reported by Ma et al. [30-31], Lee et al. [32] and Pang et al. [33] taking into account key parameters such as the mass fraction of nanoparticles and initial ammonia concentration. Some of these studies with CNTs do not include heat removal [30- 31].

Researchers have studied and discussed the mechanisms that may justify the increase in the thermal conductivity and convective heat transfer coefficient of nanofluids with respect to the base fluid [34-38]. Based on the proposed mechanisms, it is clear that heat transfer enhancement with nanofluids is not only due to the increase in thermal conductivity but also to the slip mechanisms, such as the Brownian motion, which refers to the random motion of nanoparticles, and thermophoresis caused by the temperature gradients, with the effect of the slip mechanisms being more detrimental.

Since heat and mass transfer are analogue processes, investigations on nanofluids have also showed outstanding mass transfer enhancements [27-33, 39-45]. These studies reported that possible reasons for the mass transfer enhancements in bubble absorbers are the induced micro disturbances and the increase in the gas-liquid interfacial bubble area due to motion and nanoparticles interaction. Moreover, Krishnamurthy et al. [39] showed that an optimum volume fraction of nanoparticles could result in a mass transfer enhancement higher than that observed in thermal conductivity. It is worthy of mention that because of the different operating conditions and methodologies employed in investigations dealing with mechanisms of transport phenomena in nanofluids, agreement with possible theories has not been established.

With regard to the intensification of the absorption process with the $NH_3/LiNO_3$ mixture as working pair, Oronel et al. [46] experimentally studied the absorption processes with the $NH_3/LiNO_3$ and $NH_3/(LiNO_3+H_2O)$ mixtures in a three channel plate heat exchanger with L type corrugations. In this work, the effect of the main operating conditions on absorber performance, such as solution concentration and flow rate and cooling-water flow rate and temperature, was evaluated and empirical correlations for Nusselt and Sherwood numbers of the solution were proposed on the basis of the experimental data. Recently, Amaris et al. [47] have studied the effect of inner advanced surfaces in tubular bubble absorbers in the ammonia absorption process using $NH_3/LiNO_3$ as a working

pair. Experiments in the bubble absorber with a smooth internal tube have also been performed and the results were compared with those achieved using the advanced surface tube. The absorber performance with advanced surfaces using two tube lengths (1 and 3 m) and two tube diameters (8 and 9.5 mm) have also been investigated. Results from this work have shown that the maximum absorption rate achieved with the advanced surfaces was up to 1.7 times higher than that of the smooth tube.

In the present paper, the individual and simultaneous effects of the carbon nanotubes (CNTs) and aluminum advanced surfaces on the heat and mass transfer processes in a tubular bubble absorber is experimentally studied. The $NH_3/LiNO_3$ mixture is used as a working pair, due to its promising potential for solar cooling applications. Experiments were performed in an experimental set-up under operating conditions of interest for solar air-cooled absorption refrigeration equipment.

2. Experimental procedure details

2.1 Experimental equipment

Fig. 1 shows a diagram of the experimental equipment used to study the ammonia absorption process. Measuring equipment such as RTD temperature sensors (T), pressure transducers (P), magnetic flow meters (F) and Coriolis flow meters (C) was set as shown in Fig. 1. Measuring equipment is connected to a data acquisition unit.

The experimental equipment consists mainly of three circuits: the solution circuit, the cooling-water circuit, and the heating-water circuit. The solution circuit (dark and pea green lines) comprises two stainless-steel tanks (ST1 and ST2), an electric resistance (R3), a magnetically coupled internal gear pump, a heat exchanger (SHE), a vapor-liquid separator (VLS) and the test section where the ammonia absorption process takes place. The cooling-water circuit, which allows the heat released from the absorption process to be removed, consists of a 5 kW heater (R2), a magnetic flow meter, a pump, and a heat exchanger (HX1). The heating-water circuit, which allows the solution to be heated to the required inlet thermal conditions, consists of a 5 kW heater (R1), a water-water heat exchanger (HX2), a pump and a magnetic flow meter.

2.2 Test section

The absorber, which consists of a double pipe heat exchanger, was tested with inner smooth and advanced surface tubes of 8.0 mm (outer diameter), Fig. 2. The advanced surface tube tested, supplied by Hydro, is an aluminum tube with internal helical micro-fins measuring 0.3 mm in length and a helix angle of 20º. The inner diameter of the advanced surface tube (internal equivalent diameter) was measured at the fin tip diameter. Both tubes are one meter long with a heat transfer area of 0.025 m^2, have an internal equivalent diameter of 0.006 m and an annular hydraulic diameter of 0.0025 m. The ammonia vapor and the solution flow in co-current configuration from the bottom to the top of the absorber and the cooling-water flows in counter-current through the annulus channel.

2.3 Carbon nanotubes

In order to study the effect of nanoparticles on the ammonia absorption process with the $NH_3/LiNO_3$ working pair, multi walled carbon nanotubes (CNTs) were selected. Fig. 3 shows a TEM image of the tested multi walled carbon nanotubes. CNTs have outstanding thermal and mechanical properties and it is easier for heat to move rapidly for long distances along the high-conductivity fibers (Eastman et al. [48]). Additionally, due to the fact that CNTs do not chemically react with ammonia as may happen with metal based nanoparticles (Ma et al. [41, 42] and Yang et al. [49]), CNTs seem more suitable for use in ammonia based working fluids. On the other hand, studies on the reaction of the carbon nanotubes to salts such as lithium nitrate have not been found and this should be taken into consideration for further research.

Before the CNTs were introduced into the base solution, they were subjected to a chemical treatment to achieve a better dispersion and suspension. CNTs were treated with Nitric acid (70 %) and hydrogen peroxide (35 %), and then washed with deionized water until a neutral pH-value of 7 was reached (Datsyuk et al. [50]). Fig. 4 shows a picture of the binary nanofluid with the CNTs (0.01 wt. %) added to the $NH_3/LiNO_3$ solution just after preparation and after 24 hours in a motionless state there was only a slight sedimentation. Due to the fact that during the experimental study, the CNTs – $NH_3/LiNO_3$ mixture was in constant recirculation, sedimentation was not a problem. Although sedimentation occurred several days after stopping the experimental setup, an optimum dispersion was reestablished after two hours of running. Specifications of the carbon nanotubes are summarized in Table 1.

2.4 Absorber efficiency parameters

In each experiment, once a steady-state regime was reached, measured parameters of the operating conditions were maintained and recorded for around 15 minutes.

Parameters considered to assess the absorber performance are presented below.

The ammonia absorption mass flux (F_{AB}), which quantifies the capacity of the system to absorb ammonia vapor from the evaporator, is defined as the absorbed ammonia mass flow rate per unit of heat transfer area.

$$F_{AB} = \frac{\dot{m}_{NH3,Absorbed}}{A_{Exchange}} \tag{1}$$

The absorber thermal load is determined from the measured data on the water-side.

$$Q_{AB} = \dot{m}_{Cw} \cdot Cp_{Cw} \cdot \left(T_{Cw,Out} - T_{Cw,In}\right) \tag{2}$$

The solution heat transfer coefficient (h_{Sol}) in the tubular absorber is obtained from Eq. (3).

$$\frac{1}{U \cdot D_{Outer}} = \frac{1}{h_{Sol} \cdot D_{Inner}} + \frac{Ln(D_{Outer} / D_{Inner})}{2 \cdot k_{Al}} + \frac{1}{D_{Outer} \cdot h_{Cw}} \tag{3}$$

Where the overall heat transfer coefficient U is given by Eq. (4).

$$U = \frac{Q_{AB}}{A_{Exchange} \cdot LMTD} \tag{4}$$

The cooling-water heat transfer coefficient (h_{Cw}) in the tubular absorber was determined by using Gnielinski´s well-known correlation for the Nusselt number [51], Eq. (5).

$$\mathrm{Nu}_{Cw} = \left[\frac{(f/8) \cdot (\mathrm{Re} - 1000) \cdot \mathrm{Pr}}{1 + 12.7 (f/8)^{0.5} (\mathrm{Pr}^{2/3} - 1)} \right] \cdot C \tag{5}$$

where Ci is the correction factor for flows in annular spaces, Petukhov and Royzen [52], and f is the Darcy friction factor taken from the correlation developed by Petukhov [53].

$$C = 0.86 \left(\frac{D_{Outer}}{D_{inner,o}} \right)^{-0.16} \tag{6}$$

Finally, the degree of subcooling of the solution at the absorber outlet (ΔT_{Sub}) indicates the available absorption potential.

$$\Delta T_{Sub} = (T_{Sol,Eq,Out} - T_{Sol,Out}) \tag{7}$$

where $T_{Sol,Eq,Out}$ is the equilibrium temperature of the solution at the absorber pressure and actual outlet concentration of the solution. Solution concentrations in ammonia at

the absorber inlet and outlet were determined from the density and temperature values measured by Coriolis flow meters using the density correlation reported by Libotean et al. [54].

2.5 Uncertainty determination

The method for calculating the uncertainty of the parameters described in section 2.4 is reported in Technical Note 1297 of the National Institute of Standards and Technology NIST, and implemented in the EES software (Taylor and Kuyatt [55]). Table 2 shows the error of measurement in the recorded experimental data and uncertainty of the calculated parameters under study taking into consideration a 95 % confidence interval.

3. Experimental results and discussion

Most significant results of the experimental study into the absorption process with $NH_3/LiNO_3$ fluid mixture and carbon nanotubes (CNTs) are presented below. More detailed results can be found in the PhD thesis by Amaris [56].

First shown are the experimental results achieved with a double pipe heat exchanger and smooth surface with and without CNTs into the base mixture $NH_3/LiNO_3$. Then, a comparison is made between the results of using smooth and advanced surface tubes with the base mixture and the binary nanofluid. Finally, experiments using two CNT concentrations, two cooling-water temperatures and the advanced surface tube are presented.

Table 3 shows experimental operating conditions, set due to their interest for air-cooled single-effect absorption refrigeration cycles with $NH_3/LiNO_3$ at evaporation and condensation/absorption temperatures of 5 ºC and 40 ºC, respectively.

During the experiments, the cooling water flow was kept in the transition regime in order to avoid too high an uncertainty propagation in the absorber thermal load and solution heat transfer coefficient, caused by small differences in the water-side temperature.

3.1 Effect of the multi-wall carbon nanotubes

In this subsection, the effect on the performance of the absorber by adding CNTs to the base mixture $NH_3/LiNO_3$ is analysed. The concentration of CNTs in the base mixture was initially set to 0.01 wt. %, based on previous studies in the literature dealing with the effect of CNTs on absorption capacity when added to mixtures of absorption

refrigeration cycles (Kang et al. [26] and Lee et al. [32]) and on CNT stability tests performed in our study. Experiments were carried out varying the solution mass flow and cooling-water temperature. Results are compared between the CNT binary nanofluid and base fluid mixture using the tubular absorber with an inner smooth surface.

Fig. 5 shows the trends of the absorption mass flux and solution heat transfer coefficient for the smooth tube absorber with and without nanoparticles. It is observed that by decreasing the cooling-water temperature, the ammonia absorption mass flux increases due to the fact that a wider temperature difference in the cooling-water side allows for increased heat dissipation and, therefore, higher ammonia absorption capacity. At a cooling-water temperature of 40 ºC and a solution mass flow ranging from 20 to 70 $kg.h^{-1}$, ammonia absorption mass flux of the base fluid mixture $NH_3/LiNO_3$ varied slightly between 0.0032 and 0.0035 $kg.s^{-1}m^{-2}$, however, a significant increase from 0.0038 to 0.0054 $kg.s^{-1}m^{-2}$ was observed for CNT binary nanofluid (Fig. 5a). Moreover, at a cooling-water temperature of 35 ºC, ammonia absorption mass flux varied from 0.0039 to 0.0042 $kg.s^{-1}m^{-2}$ for the base mixture and from 0.005 to 0.0063 $kg.s^{-1}m^{-2}$ for the CNT binary nanofluid. Hence, the maximum values of the absorption mass flux achieved with CNT binary nanofluid were about 1.64 and 1.48 times higher than those of the base fluid mixture at cooling-water temperatures of 40 and 35 ºC, respectively. This indicates that the effect of nanoparticles is more significant when the absorption potential is lower.

Fig. 5b shows that the solution heat transfer coefficient of base fluid mixture increased from 0.9 to a maximum of 1.78 $kW.m^{-2}K^{-1}$ and from 1.13 to 2.09 $kW.m^{-2}K^{-1}$ for CNT binary nanofluid when the solution mass flow was varied from 20 to 70 $kg.h^{-1}$. Hence, the maximum value of the solution heat transfer coefficient achieved with CNT nanofluid was about 1.29 times higher than the corresponding value for the base fluid mixture. As depicted in Fig. 5b, the effect of the cooling-water temperature on the solution heat transfer coefficient is less pronounced for both case studies.

Similarly, the absorber thermal load with CNT binary nanofluid is about 1.32 and 1.49 times higher than for the base fluid mixture at cooling-water temperatures of 40 and 35 ºC, respectively (Fig. 6a). Regarding the sub-cooling degree of the solution leaving the absorber, Fig. 6b shows that subcooling values are higher for the cooling-water temperature of 35 ºC and this parameter is hardly affected by the solution mass flow.

For the operating conditions considered in this work, subcooling values are below 6 ºC which means that the absorber operated near to its optimal capacity.

3.2 Simultaneous effect of carbon nanotubes and advanced surfaces

A comparison between the individual effect and simultaneous effect of carbon nanotubes and advanced surfaces on the absorber efficiency parameters is illustrated in Figs. 7 and 8. Specifications of the advanced surface tube used were given in sub-section 2.2. The data in these figures correspond to a CNT concentration in the base fluid mixture and a cooling-water temperature of 0.01 wt. % and 40 ºC, respectively.

Fig. 7a shows ammonia absorption mass flux achieved experimentally for the selected case studies. At low solution flows, the absorption mass flux values for the base fluid mixture $NH_3/LiNO_3$ and advanced surface tube are close to the results achieved using CNT nanofluid and a smooth tube. However, at high solution flows, the effect of the advanced surfaces on the ammonia absorption mass flux is more pronounced. Absorption mass flux values for the base mixture $NH_3/LiNO_3$ and the advanced surface tube are about 1.09 and 1.17 times higher than those achieved using CNT nanofluid and a smooth tube at solution mass flows of 40 and 50 $kg.h^{-1}$, respectively.

Regarding the simultaneous effect of the CNTs and advanced surfaces on the absorber performance, Fig. 7a shows that combining both intensification techniques resulted in a sharp increase in absorption capacity. At the selected operating conditions, ammonia absorption mass flux for the binary nanofluid and advanced surface tube ranged from 0.0041 to 0.0063 $kg.s^{-1}m^{-2}$, which represents 1.61 to 1.80 times the values achieved using the base fluid mixture $NH_3/LiNO_3$ and the smooth tube. Nevertheless, the benefit achieved by the combined effect of the carbon nanotubes and advanced surfaces is more pronounced at low solution mass flows and is gradually reduced as the solution mass flow increases approaching the results obtained with advanced surfaces without nanoparticles.

As commented previously for the absorption mass flux, the numerical values of the absorber thermal load for the case studies: (i) CNT binary nanofluid with the smooth surface tube and (ii) base fluid mixture $NH_3/LiNO_3$ with the advanced surface tube, were similar (Fig. 7b). However, the solution heat transfer coefficient values using the CNT binary nanofluid with the smooth tube were slightly lower than those of the base fluid mixture using the advanced surface tube (Fig 8a). Moreover, the simultaneous use of CNTs and advanced surface tube resulted in a more significant increase in the

absorber thermal load and solution heat transfer coefficient at high solution flow rates, which is a clear sign of a synergistic effect. Induced turbulence by micro-fins and constant nanoparticle interaction with the rough wall surface may facilitate the bubble breaking, its absorption by the solution and a significant increase in heat transfer.

Maximum values of the absorber thermal load and solution heat transfer coefficient were, respectively, about 1.35 and 1.40 times higher than the values achieved using the base fluid mixture and the advanced surface tube. The solution heat transfer improvement with the binary nanofluid is more pronounced due to an increase in the absorber thermal load and also because a lower logarithmic mean temperature difference was obtained. The subcooling degree of the solution leaving the absorber at the selected operating conditions was similar for all considered case studies and lower than 4 ºC (Fig. 8b). The improvement observed in the absorption rates using both CNTs and advanced surface tube, resulted in a higher solution concentration at the absorber exit and, therefore, a lower equilibrium temperature. Moreover, the increase in the solution heat transfer coefficient caused a decrease of the same magnitude in the actual temperature of the solution leaving the absorber, allowing the degree of subcooling of the solution to remain almost constant.

3.3 Effect of carbon nanotube concentration and cooling-water temperature

Fig. 9 shows experimental data conducted to study the effect of CNT concentration on the absorber performance using the advanced surface tube. The experiments were performed at cooling-water temperatures of 35 and 40 ºC and CNT concentrations of 0.01 and 0.02 wt. %. Higher CNT concentrations were not considered because poor stability of CNT in the base fluid mixture was observed increasing nanoparticle concentrations. Similar results for the stability of CNTs in the base fluid mixture were obtained by Cuenca et al. [57] in their study on the thermal conductivity of the $NH_3/LiNO_3$ fluid mixture with CNTs.

As observed in Fig. 9, no significant variations were obtained in the absorber performance parameters between the sets of data corresponding to CNT concentration at 0.01 and 0.02 wt. %. At a cooling-water temperature of 35 ºC, ammonia absorption mass flux increased from 0.006 to a maximum of 0.0078 $kg.s^{-1}m^{-2}$ (Fig. 9a) and the absorber thermal load increased from 6.5 to 13.4 $kW.m^{-2}$ (Fig. 9b) when the solution mass flow was varied from 15 to 65 $kg.h^{-1}$. With regard to the solution heat transfer coefficient, sets of data depicted in Fig. 9c at the selected cooling-water temperatures

and CNT concentrations have similar values and show similar trends as the solution flow increases. The solution heat transfer coefficient ranges between 1.12 and 3.65 $kW.m^{-2} K^{-1}$.

3.4 Effect of carbon nanotubes on the total pressure drop

Fig. 10 shows the pressure drop measured in the smooth tube absorber with and without CTNs and also in the advanced surface tube with and without CTNs. It is worthwhile to highlight that the presence of CNTs in the working fluid hardly affects pressure drop in the smooth tube at the selected operating conditions. It can also be observed that the total pressure drop values for the advanced surface tube with the base fluid are slightly lower than those for the smooth tube. This issue is attributed to a thinner wall thickness in the advanced surface tube in comparison with the smooth tube which in turn results in a slightly higher passage area and a lower flow velocity.

Fig. 10 also depicts that total pressure drop values for the advanced surface tube absorber with a CNT concentration of 0.01 wt. % are slightly lower than those for the smooth tube with the base mixture. However, pressure drop values for a CNT concentration of 0.02 wt. % are slightly higher than the values for the smooth tube absorber with the base mixture. According to these results, it can be expected that the total pressure drop increases for higher CNT concentrations and solution flows.

Therefore, the use of a very small fraction of CNTs in the base fluid mixture significantly enhances the heat and mass transfer processes in the absorber without penalizing the pressure drop, viscosity and density of the mixture.

4. Conclusions

In this paper, two passive techniques, namely carbon nanotubes (CNTs) and advanced surfaces, used to intensify heat and mass transfer processes in a tubular bubble absorber with $NH_3/LiNO_3$ mixture as working pair have been experimentally investigated. The individual and simultaneous effects of both techniques on the absorber efficiency parameters have been analyzed at operating conditions of interest for absorption chillers driven by low temperature heat sources. From the experimental results, the following conclusions are drawn:

- Carbon nanotubes significantly improve the ammonia absorption process in the tubular bubble absorber with the $NH_3/LiNO_3$ mixture. With respect to the reference values, maximum enhancement achieved on the absorption mass flux

with carbon nanotubes was of about 1.64 and 1.48 times at cooling-water temperature of 40 and 35 ºC, respectively, while maximum value achieved for the solution heat transfer coefficient with carbon nanotubes was around 1.39 times higher.

- The effects of the intensification techniques on heat and mass transfer processes are more pronounced as the solution mass flow increases. Moreover, it was observed that the mass fraction employed for carbon nanotubes does not affect pressure drop at the operating conditions under study.
- Regarding the simultaneous effect of carbon nanotubes and advances surfaces, experimental data showed an outstanding improvement in the absorption mass flux at low values of the solution mass flow. However, at high values of the solution mass flow, enhancement was less pronounced and the results were very close to those achieved with the base fluid mixture and advanced surfaces. Moreover, an important synergic effect was observed in the solution heat transfer coefficient.
- Absorber performance with CNT concentrations of 0.01 and 0.02 wt. % showed no significant differences. Both CNT concentrations showed good stability in the base fluid during experiments.

Acknowledgements

This study is part of an R&D project funded by the Spanish Ministry of Science and Innovation (ENE2008-00863). The authors would like to thank HYDRO for providing the advanced surface tubes. Carlos Amaris would like to thank the Spanish Ministry of Science and Innovation for the award of the scholarship (BES-2009-015241).

References

[1] K. Gensch, Lithiumnitratammoniakat als absorptionsflüssigkeit für kältemaschinen, Zeitschrift für die gesamte Kälte, Industrie, 2 (1937) 24–30.

[2] M.K. Aggarwal and R.S. Agarwal, Thermodynamic properties of lithium nitrate ammonia mixtures, Int. J. Energy Research 10(1) (1986) 59-68.

[3] C.A. Infante Ferreira, Thermodynamic and physical property data equations for ammonia-lithium nitrate and ammonia-sodium thiocyanate solutions, Solar Energy 32 (2) (1984) 231-236.

[4] K.A. Antonopoulos, E.D. Rogdakis, Performance of solar driven ammonia-lithium nitrate and ammonia-sodium thiocyanate absorption systems operating as coolers or heat pumps in Athens, Applied Thermal Engineering 16 (2) (1996) 127-147.

[5] D.W. Sun, Comparison of the performances of NH_3-H_2O, NH_3-$LiNO_3$ and NH_3-NaSCN absorption refrigeration systems, Energy Conversion Management 39 (1998) 357-368.

[6] J.M. Abdulateef, K. Sopian, M.A. Alghoul, Optimum design for solar absorption refrigeration systems and comparison of the performances using ammonia water, ammonia-lithium nitrate and ammonia-sodium thiocyanate solutions, Int. J. Mechanical and Materials Engineering 3 (1) (2008) 17-24.

[7] C.A. Infante Ferreira, Operating characteristics of NH_3-$LiNO_3$ and NH_3-NaSCN absorption refrigeration machines, Proceedings of The Nineteenth Int. Congress of Refrigeration, vol. IIIa, 1995, 321-328.

[8] R. Ayala, J.L. Frías, C.L. Heard, F.A. Holland, Experimental assessment of and ammonia/lithium nitrate absorption cooler operated on low temperature geothermal energy, Heat Recovery Systems & CHP 14 (1994) 437-446.

[9] C.L. Heard, R. Ayala, R. Best, An experimental comparison of an absorption refrigerator using ammonia/water and ammonia/lithium nitrate, Proceedings of the Int. Sorption Heat Pump Conference, Montreal, Canada, 1996, 245-252.

[10] C. Orone,l C. Amaris, M. Vallès, M. Bourouis, Experiments on the characteristics of saturated boiling heat transfer in a plate heat exchanger for ammonia/lithium nitrate and ammonia/ (lithium nitrate + water), 3rd Int. Conference on Thermal Issues in Emerging Technologies, Theory and Applications - Proceedings, art. no. 5766401, 2010, 217-225.

[11] A. Zacarías, R. Ventas, M. Venegas, A. Lecuona, Boiling heat transfer and pressure drop of ammonia-lithium nitrate solution in a plate generator, Int. J. Heat and Mass Transfer 53 (2010) 4768-4779.

[12] M. Venegas, A. Zacarías, C. Vereda, A. Lecuona, R. Ventas, Subcooled and saturated boiling of ammonia–lithium nitrate solution in a plate-type generator for absorption machines, Int. J. Heat and Mass Transfer 55 (2012) 4914-4922.

[13] J.H. Herrera, O. García-Valladares, V.H. Gómez, R. Best, Numerical simulation and experimental results of horizontal tube falling film generator working in a $NH_3/LiNO_3$ absorption refrigeration system, Applied Thermal Engineering 30 (2010) 1751-1763.

[14] M. Bourouis, A. Coronas, M. Valles, M. Zamora, Air/water or water/water absorption water cooler using ammonia and lithium nitrate, (2011), Patent PCT/ES2010/070608.

[15] W. Rivera, G. Moreno-Quintanar, C.O. Rivera, R. Best, F. Martinez, Evaluation of a solar intermittent refrigeration system for ice production operating with ammonia/lithium nitrate, Solar Energy 85 (2011) 38-45.

[16] U. Llamas, R. Best, L.A. Bujedo, P. Melogramo, N. Velazquez, I. Pilatowsky, V.H. Gomez, O. Garcia-Valladares, R. Fedrizzi, A. Corredera, J.I. Hernandez, S. Sanz, A. Ortega, First experimental results of a solar driven ammonia-lithium nitrate cooling system, 4th Int. Conference Solar Air-Conditioning, 2011, Nikosia, Cyprus.

[17] A. Zacarías, M. Venegas, R. Ventas, A. Lecuona, Experimental assessment of ammonia adiabatic absorption into ammonia-lithium nitrate solution using a flat fan nozzle, Applied Thermal Engineering 31 (2011) 3569-3579.

[18] R. Ventas, C. Vereda, A. Lecuona, M. Venegas, M.C. Rodríguez-Hidalgo, Effect of the NH_3-$LiNO_3$ concentration and pressure in a fog-jet spray adiabatic absorber, Applied Thermal Engineering 37 (2012) 430-437.

[19] A. Zacarías, M. Venegas, A. Lecuona, R. Ventas, Experimental evaluation of ammonia adiabatic absorption into ammonia-lithium nitrate solution using a fog jet nozzle, Applied Thermal Engineering 50 (2013) 781-790.

[20] G. Moreno-Quintanar, W. Rivera, R. Best, Comparison of the experimental evaluation of a solar intermittent refrigeration system for ice production operating with the mixtures $NH_3/LiNO_3$ and $NH_3/LiNO_3/H_2O$, Renewable Energy 38 (1) (2012) 62-68.

[21] Y. T. Kang, A. Akisawa, T. Kashiwagi, Experimental correlation of combined heat and mass transfer for NH_3–H_2O falling film absorption, Int. J. Refrigeration 22 (1999) 250–262.

[22] J. Cerezo, R. Best, M. Bourouis, A. Coronas, Comparison of numerical and experimental performance criteria of an ammonia–water bubble absorber using plate heat exchangers, Int. J. Heat and Mass Transfer 53 (2010) 3379–3386.

[23] W.A. Miller, The synergism between heat and mass transfer additive and advanced surfaces in aqueous LiBr horizontal tube absorbers, Proceedings of the Int. Sorption Heat Pump Conference, Munich, Germany,1999.

[24] J.I. Yoon, E. Kim, K.H. Choi, W.S. Seol, Heat transfer enhancement with a surfactan on horizontal bundle tubes of an absorber, Int. J. Heat and Mass Transfer, 45 (2002) 735-741.

[25] C.W. Park, H.C. Cho, Y.T. Kang, The effect of heat transfer additive and surface roughness of micro-scale hatched tubes on absorption performance, Int. J. Refrigeration 27 (2004) 264-270.

[26] Y. T. Kang, H. J. Kim, K. I. Lee, Heat and mass transfer enhancement of binary nanofluids for H_2O/LiBr falling film absorption process, Int. J. Refrigeration, 31 (2008) 850-856.

[27] H. Kim, J. Jeong, Y. T. Kang, Heat and mass transfer enhancement for falling film absorption process by SiO_2 binary nanofluids, Int. J. Refrigeration 35 (2012) 645-651.

[28] J-K. Kim, J. Y. Jung, Y. T. Kang, The effect of nano-particles on the bubble absorption performance in a binary nanofluid, Int. J. Refrigeration, 29 (2006) 22-29.

[29] J-K. Kim, J. Y. Jung, Y. T. Kang, Absorption performance enhancement by nano-particles and chemical surfactants in binary nanofluis, Int. J. Refrigeration, 30 (2007) 50-57.

[30] X. Ma, F. Su, J. Chen, Y. Zhang, Heat and mass transfer enhancement of the bubble absorption for a binary nanofluids, J. Mechanical Science and Technology 21 (2007) 1813-1818.

[31] X. Ma, F. Su, J. Chen, T. Bai, Z. Han, Enhancement of bubble absorption process using a CNTs-ammonia binary nanofluid, Int. Commun. Heat and Mass Transfer, 36 (2009) 657–660.

[32] J. K. Lee, J. Koo, H. Hong, Y. T. Kang, The effects of nanoparticles on absorption heat and mass transfer performance in NH_3/H_2O binary nanofluids, Int. J. Refrigeration 33 (2010) 269-275.

[33] C. Pang, W. Wu, W. Sheng, H. Zhang, Y. T. Kang, Mass transfer enhancement by binary nanofluids (NH_3/H_2O + Ag nanoparticles) for bubble absorption process, Int. J. Refrigeration 35 (8) (2012) 2240-2247.

[34] P. Keblinski, S.R. Phillpot, S.U.S. Choi, J.A. Eastman, Mechanism of heat flow in suspensions of nano-sized particles (nanofluids), Int. J. Heat and Mass Transfer 45 (2002) 855-863.

[35] S. Das, N. Putra, P. Thiesen, W. Roetzel, Temperature dependence of thermal conductivity enhancement for nanofluids, Journal of Heat Transfer 125 (2003) 567-574.

[36] J. Buongiorno, Convective transport in nanofluids, J. Heat Transfer, 128 (2006) 240–250.

[37] Z. Haddad, E. Abu-Nada, H. F. Oztop, A. Mataoui, Natural convection in nanofluids: Are the thermophoresis and Brownian motion effects significant in nanofluid heat transfer enhancement?, Int. J. Thermal Sciences, 57 (2012) 152–162.

[38] Y. Ding, H. Chen, Y. He, A. Lapkin, M. Yeganeh, L. Siller, Y. V. Butenko, Forced convective heat transfer of nanofluids, Advanced Powder Technology 18 (6) (2007) 813–824.

[39] S. Krishnamurthy, P. Bhattacharya, P. E. Phelan, Enhanced mass transport in nanofluids, Nano Letters 6 (3) (2006) 419-423.

[40] V. Linek, M. Korda, M. Soni, Mechanism of gas absorption enhancement in presence of fine solid particles in mechanically agitated gas–liquid dispersion. Effect of molecular diffusivity, Chemical Engineering Science 63 (2008) 5120-5128.

[41] X. Fang, Y. Xuan, Q. Li, Experimental investigation on enhanced mass transfer in nanofluids, Applied Physics Letters 95 (2009) 203108.

[42] J. Veilleux, S. Coulombe, A dispersion model of enhanced mass diffusion in nanofluids, Chemical Engineering Science 66 (2011) 2377–2384.

[43] J. W. Lee, J-Y. Jung, S-G. Lee, Y. T. Kang, CO_2 bubble absorption enhancement in methanol-based nanofluids, Int. J. Refrigeration 34 (2011) 1727-1733.

[44] I. Torres Pineda, J. W. Lee, I. Jung, Y. T. Kang, CO_2 absorption enhancement by methanol-based Al_2O_3 and SiO_2 nanofluids in a tray column absorber, Int. J. Refrigeration 35 (2012) 1402-1409.

[45] J. W. Lee and Y. T. Kang, CO_2 absorption enhancement by Al_2O_3 nanoparticles in NaCl aqueous solution, Energy 53 (2013) 206-211.

[46] C. Oronel, C. Amaris, M. Bourouis, M. Vallès., Heat and mass transfer in a bubble plate absorber with $NH_3/LiNO_3$ and $NH_3/(LiNO_3+H_2O)$ mixtures, Int. J. Thermal Sciences 63 (2013) 105-114.

[47] C. Amaris, M. Bourouis, M. Vallès, Effect of advanced surfaces on heat and mass transfer processes in a tubular bubble absorber with $NH_3/LiNO_3$ for absorption refrigeration cycles, 10th IIR Gustav Lorentzen Conference on Natural Refrigerant, June, 2012, Delft, The Netherlands.

[48] J.A. Eastman, S.R. phillpot, S.U.S. Choi, P. Keblinski, Thermal transport in nanofluids, Annual Review of Materials Research 34 (2004) 219-246.

[49] L. Yang, K. Du, S. Bao, Y. Wu, Investigations of selection of nanofluids applied to the ammonia absorption refrigeration systems, Int. J. Refrigeration 35 (2012) 2248-2260.

[50] V. Datsyuk, M. Kalyva, K. Papagelis, J. Parthenios, D. Tasis, A. Siokou, I. Kallitsis, C. Galiotis, Chemical oxidation of multiwalled carbon nanotubes, Carbon 4 (6) (2008) 833-840.

[51] V. Gnielinski, New equations for heat and mass transfer in turbulent pipe and channel flow, Int. Chemical Engineering 16 (1976) 359–368.

[52] B. S. Petukhov and L. I. Roizen, Generalized Relationships for Heat Transfer in a Turbulent Flow of a Gas in Tubes of Annular Section, High temperature 2 (1964) 65–68.

[53] B.S. Petukhov, Heat transfer and friction in turbulent pipe flow with variable physical properties, Advances in Heat Transfer 6 (1970) 503-564.

[54] S. Libotean, A. Martin, D. Salavera, M. Valles, X. Esteve, A. Coronas, Densities, viscosities, and heat capacities of ammonia + lithium nitrate and ammonia + lithium nitrate + water solutions between (293.15 and 353.15) K, J. Chemical and Engineering Data 53 (10) (2008) 2383-2388.

[55] B.N. Taylor, C.E. Kuyatt, Guidelines for Evaluating and Expressing the Uncertainty of NIST Measurement Results, National Institute of Standards and Technology Technical Note 1297, 1994.

[56]. C. Amaris, Intensification of NH_3 bubble absorption process using advanced surfaces and carbon nanotubes for $NH_3/LiNO_3$ absorption chillers, PhD Thesis, Rovira i Virgili University, Tarragona, Spain, 2013.

[57] Y. Cuenca, A. Vernet, M. Vallès, Enhanced thermal conductivity of new working fluid (NH_3 + $LiNO_3$) using CNTs binary nanofluid, Int. Workshop on New Working Fluids for Absorption Heat Pumps and Refrigeration Systems, Eurotherm Seminar nº 100, July, 2013, Tarragona, Spain.

Table 1 - Specifications of the carbon nanotubes.

Multi Walled Carbon Nanotubes	
Nanoparticles supplier	Cheap Tubes inc.
Outer Diameter	20-30 nm
Inside Diameter	5-10 nm
Purity	>95 wt. %
Bulk density	0.28 g.cm^{-3}
Length	10-30 μm

Table 2 - Experimental uncertainty.

Parameters	**Uncertainty**
Sensors	
Temperature, T (ºC)	± 0.1
System pressure, P (%)	± 0.25
Solution mass flow rate, m (%)	± 0.1
Solution density, ρ(kg.m^{-3})	± 0.5
Coolant flow rate, V_{CW} (l.h^{-1})	± 0.24
Tubular Absorber	
Tube diameters, mm	0.02
Tube Length	± 0.5 %
Calculated parameters	
NH_3 absorption mass flux, F_{AB}	± 7.1 %
Absorber thermal load, Q	± 13.6 %
Solution heat transfer coefficient, h_{Sol}	± 17.0 %

Table 3 - Experimental operating conditions.

Parameters	**Range**
Solution temperature at the absorber inlet, °C	45
Cooling-water temperature at the absorber inlet, °C	35.0-40.0
Ammonia mass fraction of the solution at the absorber inlet,	0.452
Absorber pressure, kPa	510
Solution mass flow rate, kg/h	10.0-72.0
Cooling-water flow rate in the tubular absorber, l/h	80-100
Carbon nanotubes concentration in the solution, wt. %	0.00-0.02

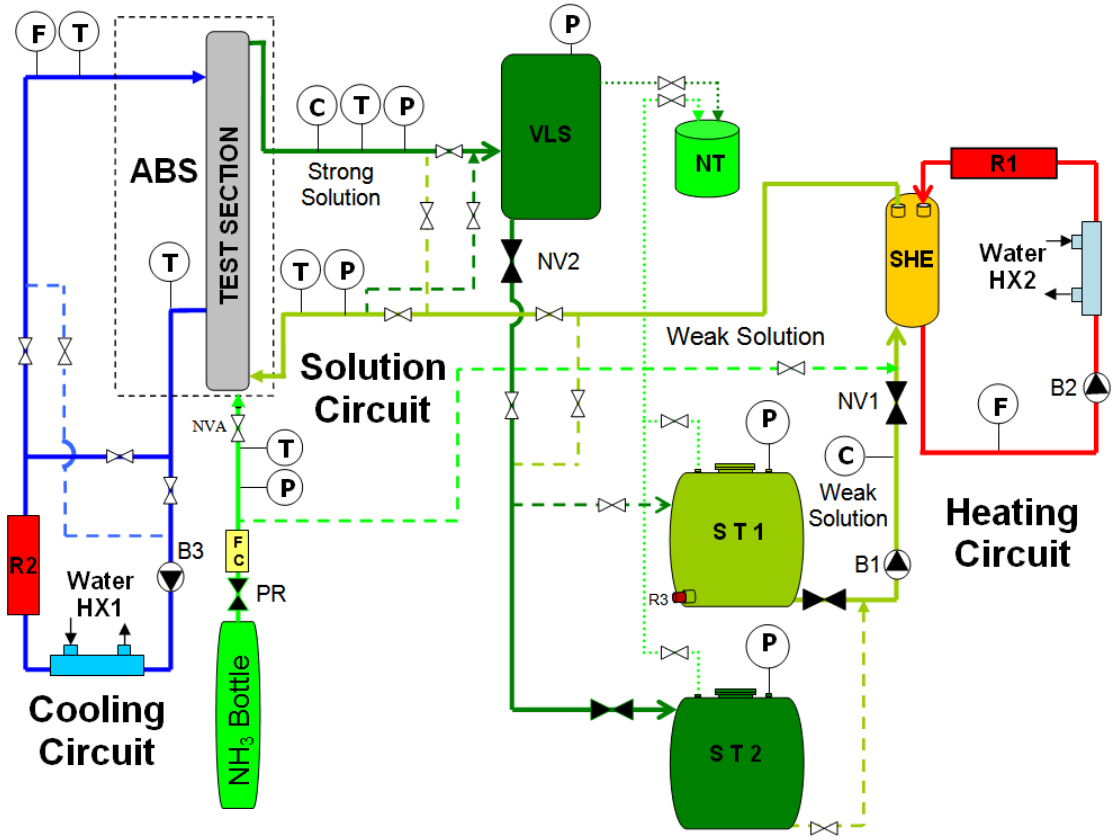

Fig. 1 - Diagram of the experimental equipment

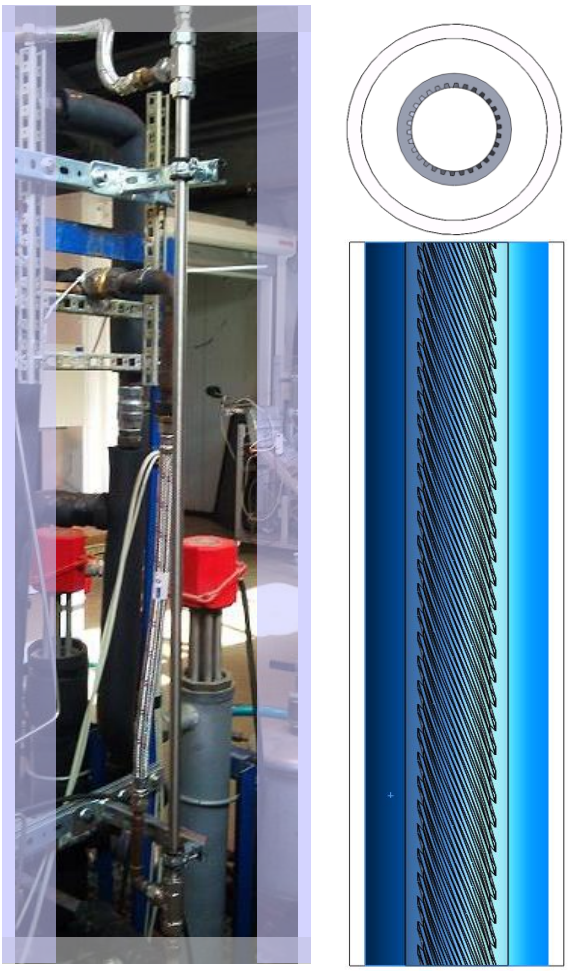

Fig. 2 - Tubular absorber test section and cross-section view of the advanced surface tube.

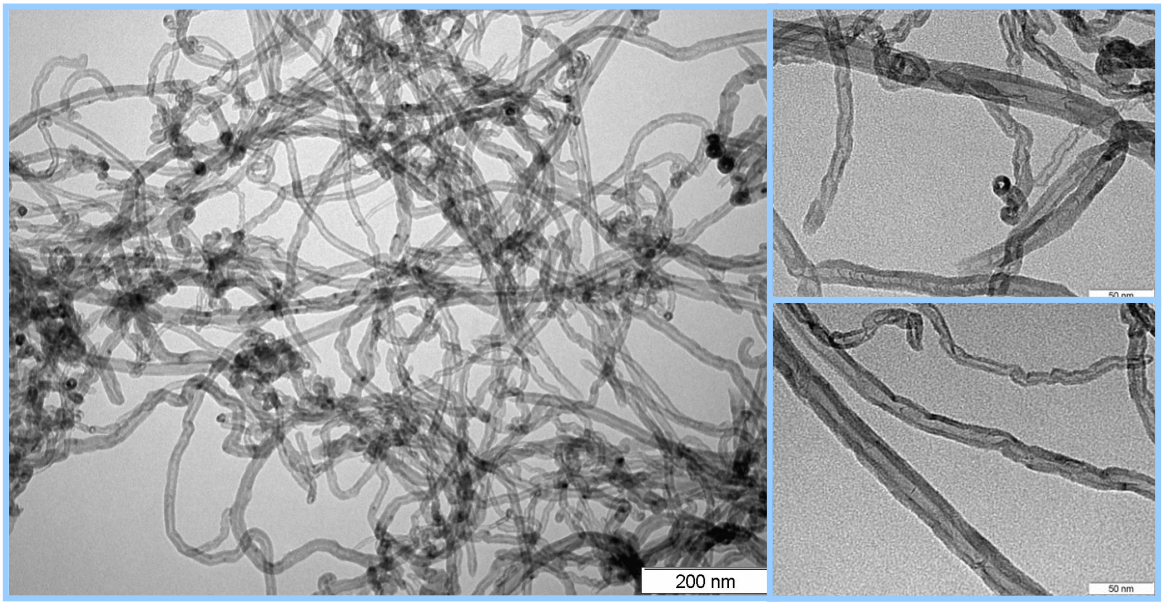

Fig. 3 - TEM picture of the tested carbon nanotubes.

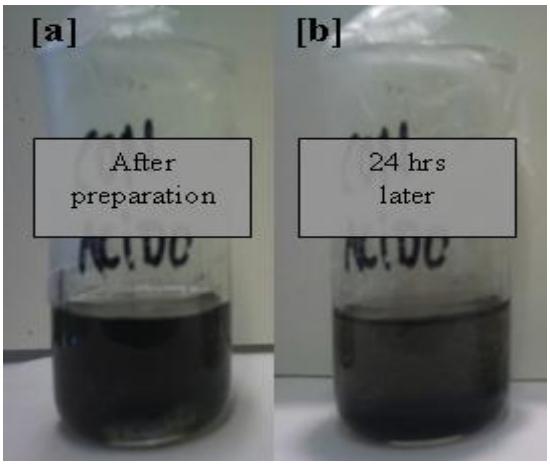

Fig. 4 - CNTs into the base fluid mixture $NH_3/LiNO_3$.

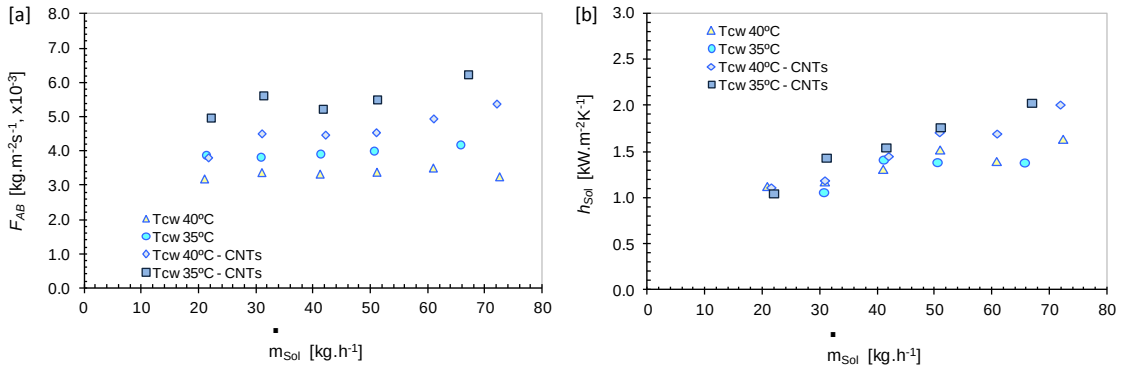

Fig. 5 - Effect of carbon nanotubes on: [a] NH_3 absorption mass flux and [b] solution heat transfer coefficient.

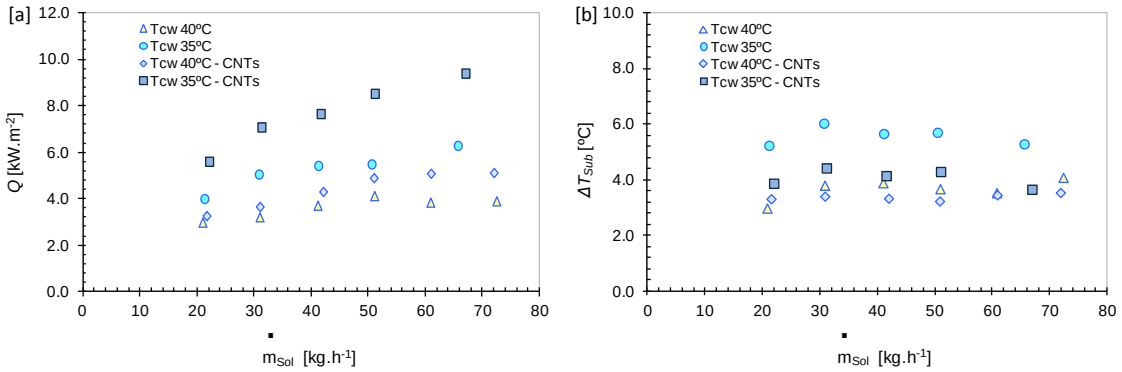

Fig. 6 - Effect of carbon nanotubes on: [a] absorber thermal load [b] degree of subcooling.

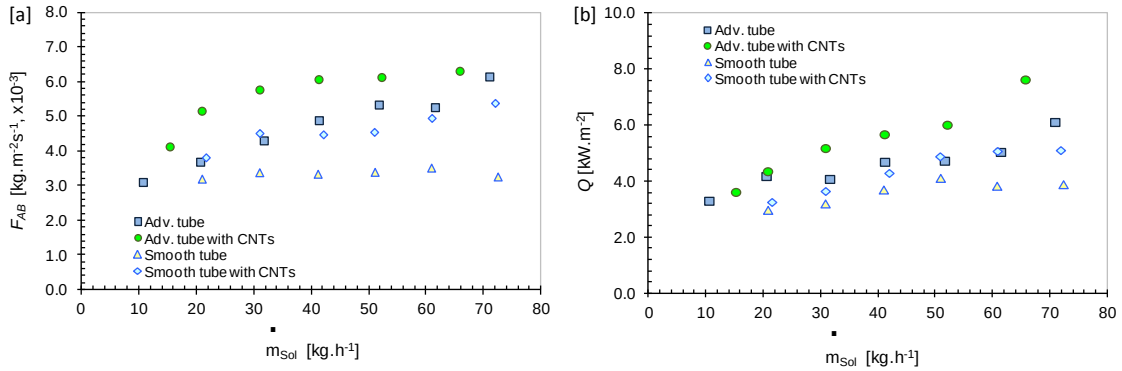

Fig. 7 - Effect of carbon nanotubes and advanced surfaces on: [a] NH_3 absorption mass flux and [b] absorber thermal load.

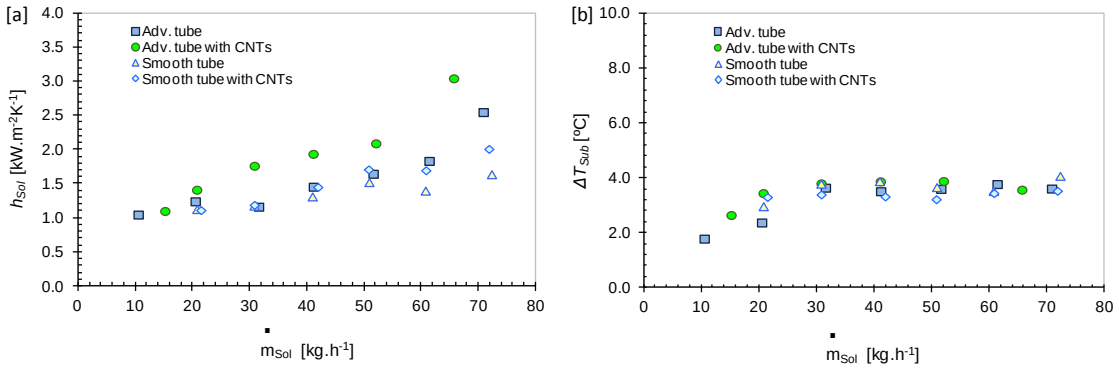

Fig. 8 - Effect of carbon nanotubes and advanced surfaces on: [a] solution heat transfer coefficient and [b] degree of subcooling.

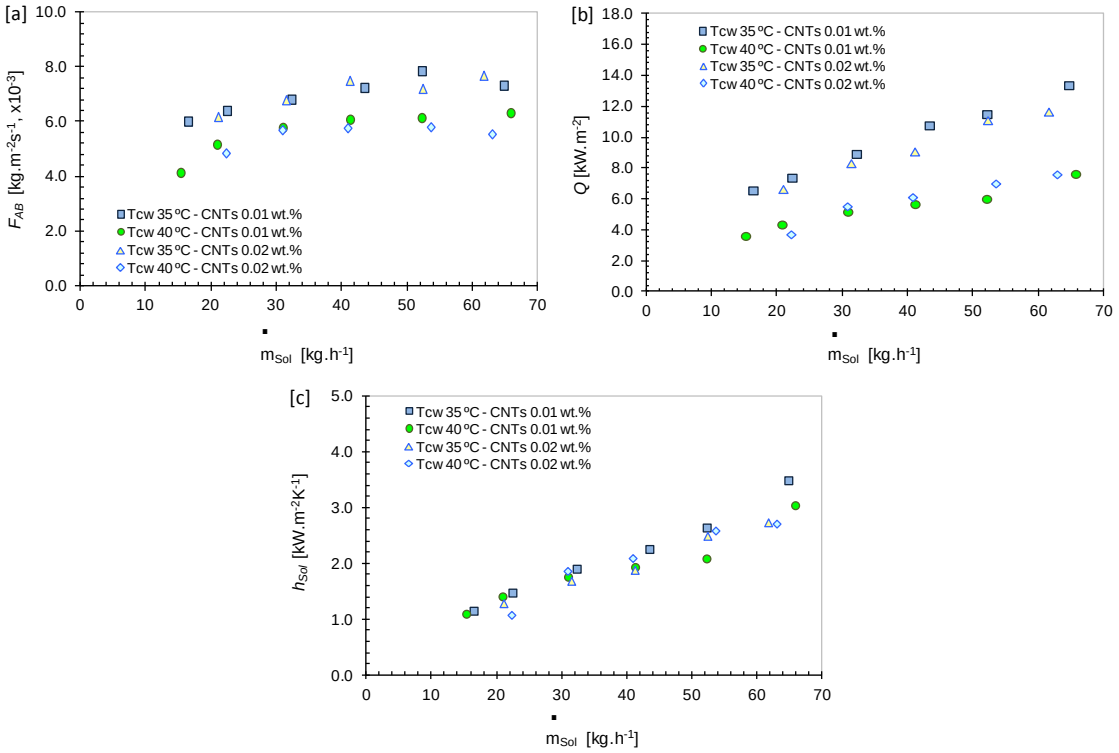

Fig. 9 - Effect of carbon nanotubes concentration and cooling-water temperature on: [a] NH_3 absorption mass flux, [b] absorber thermal load and [c] solution heat transfer coefficient.

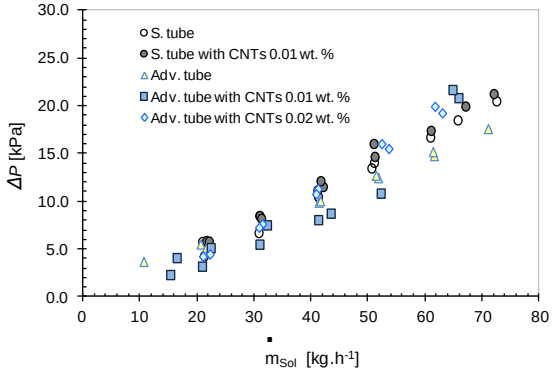

Fig. 10 - Effect of carbon nanotubes on the total pressure drop.